Polymer 123 (2017) 203–210

Contents lists available at ScienceDirect

Polymer

journal homepage: www.elsevier.com/locate/polymer

Metallic-like thermal conductivity in a lightweight insulator: Solid-state processed Ultra High Molecular Weight Polyethylene tapes and films

Sara Ronca [a, *], Tamito Igarashi [a, b], Giuseppe Forte [a], Sanjay Rastogi [a, c]

[a] Department of Materials, Loughborough University, Loughborough LE11 3TU, UK
[b] Kureha Corporation, 3-3-2, Nihonbashi Hamacho, Chuo-ku, Tokyo 103-8552, Japan
[c] Department of Biobased Materials, Faculty of Humanities and Sciences, Maastricht University, Brightlands Chemelot Campus, Urmonderbaan 22, 6167RD Geleen, The Netherlands

ARTICLE INFO

Article history:
Received 30 May 2017
Received in revised form
29 June 2017
Accepted 9 July 2017
Available online 10 July 2017

Keywords:
Oriented UHMWPE
Thermal conductivity
Laser-flash thermal analysis

ABSTRACT

Ultra High Molecular Weight Polyethylene with a reduced number of entanglements can be stretched in the solid state both uni- or biaxially to produce highly oriented tapes and films. The chain orientation, in combination with the reduced number of chain ends, is responsible for the high tensile modulus and tensile strength of the drawn materials, and, as we report here, also for the high thermal conductivity achieved through lattice movements. A property such as thermal conductivity in an electrical insulator makes UHMWPE tapes and films of great applicative interest. In-plane laser-flash thermal analysis has been applied to measure the thermal diffusivity of samples of different molecular weights stretched both uni- and biaxially, and a strong correlation has been found between the drawing ratio and the resulting in-plane thermal conductivity. Values of at least 40 W/m K have been achieved for UHMWPE having M_w comprised between 2 and 10 million, while higher values of 65 W/m K are observed for the higher M_w samples having relatively lesser number of chain ends. Surprisingly the biaxially stretched samples also show in-plane conductivity, with the highest value reaching 18 W/m K, comparable to stainless steel.

1. Introduction

Heat transfer in any material can happen by particle collisions and/or lattice vibrations, where the first mechanism is usually more effective than the latter. In metallic solids, collisions between the free electrons allow for a very efficient transfer of heat. The same free electrons are also responsible for the conduction of electricity, thus making metals both thermally and electrically conductive. In non-metallic solids, the transfer of heat can only happen through lattice vibrations, described in terms of phonons, and it is (usually) less efficient than in metals, making these materials thermally non-conducting.

Thermal conductivities (***k***) of commonly used materials, defined as the ability of a material to conduct heat, can span several orders of magnitude, from 0.024 W/m K of air to 450 W/m K of silver. Bulk polymers are usually found on the lower-end of this range [1], with values up to 1 W/m K: polyolefins, which are based on just carbon and hydrogen atoms, normally have values below 0.5 W/m K. With the addition of suitable amounts of thermally conductive fillers, polymer composites that are thermally conductive but still electrically insulating have been realized to be used in various industrial applications including circuit boards in power electronics, heat exchangers, and electronic appliances. However, these composites usually require high loading of fillers to achieve practical values of conductivity, due to a large interfacial thermal resistance (Kapitza resistance) between the filler and the surrounding polymer matrix [2]. This constitutes a significant processing challenge and also poses serious problems for recycling of the material after use.

One of the best thermal conductors known is a non-metallic material: a natural, single crystal of diamond having thermal conductivity [3] of 2190 W/m K. The high thermal conductivity is attributed to the very efficient transmission of heat through the lattice vibrations in a perfect crystal. This suggests that in principle (semi) crystalline polymers could also have high thermal conductivities, provided that the lattice vibrations could be transmitted 'unperturbed' along the chains. This condition is not met in bulk

* Corresponding author.
E-mail address: s.ronca@lboro.ac.uk (S. Ronca).

http://dx.doi.org/10.1016/j.polymer.2017.07.027

polymers (even if semi-crystalline) because of the random size, orientation and distribution of the crystalline domains and the presence of the non-crystalline component. However, the situation changes when the chains get aligned and packed in larger well oriented crystalline domains.

This concept was reported for the first time by Gibson et al. [4] in 1977 on linear polyethylene (PE). Linear polyethylene represents the best choice in terms of structure, being formed by a simple repetition of CH_2 units, with virtually no branching. The authors measured the thermal conductivity of extruded samples of PE at 100 K: these samples showed thermal conductivity anisotropy in the directions parallel ($\boldsymbol{k}_{\parallel}$) and perpendicular ($\boldsymbol{k}_{\perp}$) to extrusion, with the $\boldsymbol{k}_{\parallel}$ reaching values (~9 W/m K) comparable to stainless steel at an extrusion ratio of 25. They also observed that thermal conductivity $\boldsymbol{k}_{\parallel}$ and tensile modulus $\boldsymbol{E}_{\parallel}$ increased with draw ratio. The authors related the improvement in both mechanical and electrical properties to the alignment of chains and reduction of the amorphous component. These results suggested that, a material virtually 'free' of crystal defects where chains can be aligned at the macroscopic level should be able to provide higher values of $\boldsymbol{k}_{\parallel}$. This hypothesis has been recently confirmed by Shen et al. [5], by drawing a nanofibre of Ultra-High Molecular Weight Polyethylene (UHMWPE) with $\boldsymbol{k}_{\parallel}$ = 104 W/m K, higher than metals such as platinum, iron and nickel. A similar concept has been applied by Lu et al., achieving conductivity of 29 W/m K in a sample of electrospun polyethylene oxide [6].

The order of magnitude difference observed by Shen can be ascribed to the higher molecular weight of the polymer used (resulting in fewer chain ends that act as chain defects in the alignment) and the single-crystal nature of the nanosized fibre. Due to the dimension of the sample, a technique based on AFM had to be developed to measure the thermal properties in the range of 100 nm. It is important to notice that the work by Shen et al. conclusively demonstrated the potential of high thermal conducting polyolefin in a localised region, where the crystalline defects are restricted and chain ends are not influencing the outcome.

The study from Shen was conducted on commercial UHMWPE that, due to the multi-site nature [7] of the catalytic system and synthetic procedure used in its production, shows both a very high number of entanglements between the chains (thus requiring the formation of dilute solutions in suitable solvents to 'disentangle' the chains prior to orientation) and a very large molecular weight distribution (resulting in a distribution of chain sizes and so a more 'defective' structure of the resulting crystals). To overcome the issue of entanglements and create the oriented structure, solution spinning was adopted that required conversion of 5 wt% of the polymer using 95 wt% of the solvent.

We have previously reported that by controlled synthesis [8] it is possible to synthesize linear UHMWPEs with a reduced number of entanglements: this 'disentangled' UHMWPE can be processed in the solid state through compaction followed by stretching either uni- or bi-axially. Moreover, our synthetic method relies on the use of a different catalytic system (single-site instead of multi-site), thus ensuring a narrower distribution of chain sizes (compared to the normally used Z-N catalyst for the industrial synthesis) and the possibility to tailor the molecular weight simply by changing the reaction time.

2. Experimental methods

2.1. Materials

The UHMWPEs used for the analysis were synthesized according to Ref. [8]. Weight average molecular weight (M_w) and molecular weight distribution (MWD) for all samples have been determined using rheological measurements, as described previously [9]. For simplicity, the samples are coded as **PE_X_Y** where X is the M_w and Y is the MWD in the first significant figure. The molecular features of **PE 2_4** are: $M_w = 1.5 \times 10^6$ g/mol and MWD = 4.2; for **PE 6_7**: $M_w = 6.4 \times 10^6$ g/mol and MWD = 6.8; for **PE 10_7**: $M_w = 10 \times 106$ g/mol, MWD = 6.6.

2.2. Uniaxial stretching of UHMWPE

To achieve high orientation in the UHMWPE samples, a two-step process has been used, with an initial rolling step followed by a stretching step. Samples were sintered at 125 °C for 25min, below the melting temperature of nascent UHMWPE (~141 °C), to ensure that the disentangled character is retained. The as-sintered samples had lateral dimensions of 120 × 120 mm and 0.7 mm thickness for the samples that are rolled up to 5 times their initial length, or the samples having thickness of 1.4 mm are rolled up to 6 times the initial length. The rolling step is performed between two roll mills at 125 °C and it is repeated several times with decreasing the gap in each step, to achieve the desired value of draw ratio, defined as the ratio between the length of the sample before and after rolling of the sintered sample. After the consecutive rolling steps, the rolled tapes were cut into specimen of 100 mm length and 55 mm width and marked every 5 mm. These specimens are further stretched uniaxially with a Hounsfield tensometer, equipped with an ambient chamber set at 125 °C, from 60 mm of gauge length at 60 mm/min. Stretching is again repeated several times to achieve the desired value of elongation ratio, defined as the ratio between the length of the stretched specimen and that of the rolled specimen. Samples for thermal diffusivity measurement were cut from the middle part of the rolled-stretched specimen.

2.3. Biaxial stretching of UHMWPE

Sintered samples of 0.7 mm thickness are prepared as described for the uniaxial stretching. They are then rolled between two roll mills at 130 °C several times in different directions (vertical, horizontal, and diagonal) until the area had extended up to twice. The rolled tapes are then cut into squares with length of 120 mm and grid lines are drawn at 5 mm apart. Samples are stretched biaxially from 100 mm of gauge length at 50 mm/min by using an Instron tensometer equipped with a biaxial stretching unit, as described in Ref. [10], where the chamber temperature is set at 132 °C. Samples for evaluation are cut from the middle part of the tapes and stretching ratio is calculated from the grids lines.

2.4. Laser-flash thermal analysis

Laser-flash thermal analysis is successfully applied to measure thermal properties of materials such as thermal diffusivity and thermal conductivity: Santos and co-workers have shown that this technique can be suitably used to assess the thermal properties of polymeric materials [11].

The technique was introduced for the first time in 1961 by Parker et al. [12]: short pulses of heat are sent to the front of a specimen, while recording the temperature increase at the back of the sample. Using the half time ($t_{1/2}$, time value at half signal height) and sample thickness (d), the thermal diffusivity (α, expressed in m^2/s) can be measured according to equation (1):

$$\alpha = 0.1388 \frac{d^2}{t_{1/2}} \tag{1}$$

From the thermal diffusivity, the thermal conductivity k (in W/m K) can be calculated according to equation (2):

$$\alpha = \frac{k}{\rho c_p} \quad (2)$$

Where ρ is the material bulk density in kg/m^3 and c_p is the specific heat in J/kg K. The method gives a direct measurement of the thermal diffusivity, while the conductivity is obtained indirectly.

The measurements, as described above, are commonly used to measure the thermal diffusivity through an ideally isotropic sample: for samples of anisotropic nature, a variation of this basic set-up is applied, namely an in-plane type of measurement. The sample placed in an in-plane holder receives the heat pulse in the centre of the front side and the energy output is read through a mask placed on the back side of the sample, as shown in Fig. 1. The experimentally obtained time-temperature profile is compared with the theoretically calculated profile and the thermal diffusivity is determined. Then the in-plane thermal conductivity (k_{ip}) can be calculated.

2.5. Comparison of in-plane measurement and through-plane measurement on stacked sheets (lamellar method)

The theoretical model used for in-plane measurement takes into account the influence of anisotropy between radial direction and normal direction to the film surface. However, the uniaxially stretched films have a higher thermal conductivity in the stretching direction ($\mathbf{k}_{\parallel}$) than perpendicular to the stretching direction ($\mathbf{k_{tp}}$ for through-plane direction, $\mathbf{k}_{\perp}$ for planar direction). When $\mathbf{k}_{\parallel}$ is much higher than $\mathbf{k_{tp}}$ and $\mathbf{k}_{\perp}$, the diffusion behavior is similar to one-dimension diffusion. IR signal at the early stage of diffusion reflects the contribution mainly in the stretching direction, resulting in a good approximation of $\mathbf{k}_{\parallel}$.

Alternatively, $\mathbf{k}_{\parallel}$ can be evaluated by through-plane measurement in parallel to the stretching direction on a sample prepared by stacking multiple sheets, a method commonly defined as lamellar method. However, this method requires the stacking and alignment of many pieces of sheet to obtain a specific width of sample, especially for high TDR, and ultra-stretched UHMWPE sheet is so tough, that the cutting process may damage the specimen surface and influence the evaluation by lamellar method. Sample preparation process is less influential for in-plane measurements, so they have been preferred in this study for the purpose of comparing samples with different TDRs and molecular weights.

To validate the application of in-plane thermal conductivity measurement as a measure of $\mathbf{k}_{\parallel}$, thermal conductivities measured by lamellar-method and in-plane measurement have been compared. In-plane measurements give slightly lower values than the lamellar method because of the theoretical model assumption and the influence of sample preparation, but its correspondence is deemed to be satisfactory, as it can be appreciated from Fig. 2 below.

2.6. Through-plane thermal diffusivity measurements

Samples were cut into squares of 11 mm length. The squares were covered with Graphite spray and placed into through-plane holders. Sample's heat diffusivity was measured at 25 °C using Netzsch LFA447 laser flash apparatus and analysed using Proteus Analysis 7.0 using a Cowan + pulse correction model.

Thermal diffusivity measurements by lamellar method were performed on a selection of samples for the comparison with in-plane thermal conductivity. Multiple pieces of sample were

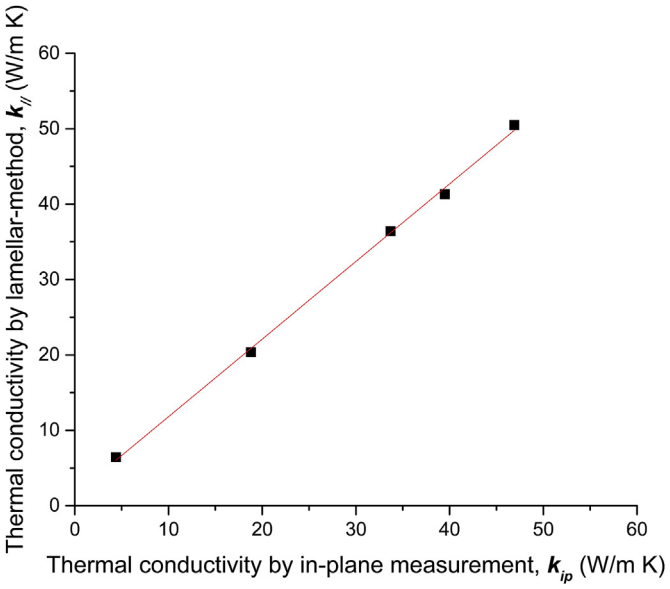

Fig. 2. Comparison between thermal conductivities measured by lamellar and in-plane methods.

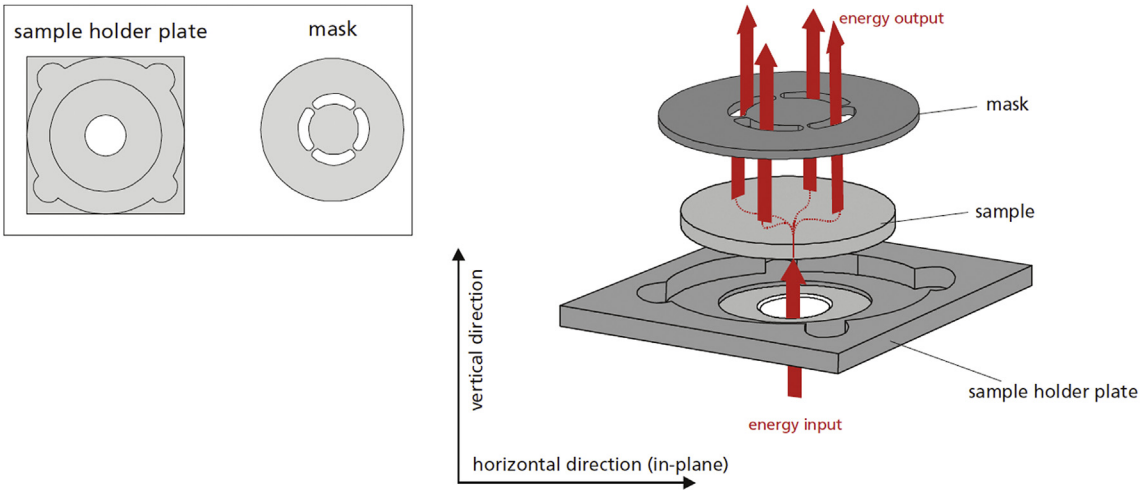

Fig. 1. In-plane holder for measurements of in-plane diffusivity of anisotropic samples (Image courtesy of Netzsch).

stacked parallel to the drawing direction to obtain slab shaped specimen. The top and bottom face, which were perpendicular to the drawing direction, were trimmed and treated with Graphite spray.

2.7. In-plane thermal diffusivity measurements

Samples were cut into circular shapes with a minimum diameter of 22 mm, placed into in-plane holders and treated with Graphite spray. Samples' heat diffusivity was measured at 25 °C using Netzsch LFA447 laser flash apparatus and analysed using Proteus Analysis 7.0; using an anisotropic, in-plane + heat loss model. The thermal conductivity was calculated using a bulk density value of $\rho = 970$ kg/m^3 and specific heat capacity of polyethylene from Ref. [13].

2.8. Differential scanning calorimetry (DSC)

DSC experiments were performed using TA instruments Q2000, which was calibrated by Indium. Samples of 0.8–1.2 mg mass were weighed and sealed into Tzero Aluminium pans. Constant heating rate experiments were performed at 10 °C/min from 30 °C to 210 °C under a Nitrogen atmosphere with a flow rate of 50 ml/min.

2.9. X-ray diffraction (XRD)

XRD experiments were performed in Bragg-Brentano geometry using a Bruker D2 Phaser diffractometer. Continuous scans were performed from 10° to 40°(2θ) at step width of 0.02° while rotating the specimen around the specimen surface normal. Peak areas of 110 and 200 reflections were estimated from XRD spectrum with corrections for polarization and irradiated volume.

3. Results and discussion

In the uniaxial drawn tapes of UHMWPE, the bundles of fibres align themselves in a preferred crystal plane orientation accounting for extraordinary high tensile modulus/strength. We have reported [14] values above 4.0 GPa for tensile strength and 200 GPa for the tensile modulus of the uniaxial stretched tapes.

The high orientation, combined with high number average molar mass ($M_n > 1 \times 10^6$ g/mol), is not only responsible for the high modulus/strength in tapes, but it has the potential to provide unique physical properties, such as thermal conductivity through lattice vibrations. To prove this possibility, we have realized a series of UHMWPE tapes varying in molecular weight/distribution and degree of stretching, realized both uniaxial and bi-axial, and we have evaluated the thermal conductivity by means of the laser-flash thermal analysis apparatus described in the experimental section.

To evaluate the influence that the two different processing steps (rolling and stretching) have on the polymer chain orientation, a sample having weight average molecular weight $M_w = 6.4 \times 106$ g/mol and a molecular weight distribution, MWD = 6.8 has been subjected to different ratios of rolling and stretching. For simplicity, the PE samples studied in this paper will be indicated as **PE_X_Y**, where X is the M_w and Y the MWD to the nearest integer. In Table 1 are reported the values of in-plane thermal conductivity ($\boldsymbol{k_{ip}}$) of **PE_6_7** calculated from the directly measured diffusivity values. We should take into account that the value measured with the in-plane technique should in principle be an average of the in-plane conductivity parallel to the chain direction and in-plane conductivity perpendicular to the chain direction. However, the in-plane conductivity perpendicular to the chain direction does not differ substantially from the through plane value (~0.2–0.3 W/mK), and the value of thermal conductivity we read, k_{ip} is basically dominated by the in-plane conductivity parallel to the chain direction. To further confirm this, we have performed through-plane measurements on stacked sheets of stretched samples, as described in the experimental section. The 'total draw ratio' (TDR) is defined as the product (rolling ratio × stretching ratio) [15,16].

When the results are plotted as thermal conductivity versus total draw ratio (Fig. 3), the data points follow a trend, suggesting that the final orientation achieved is not dependent on the individual values of rolling and stretching, but only on the TDR. This result has proved particularly valuable to achieve higher draw ratios without the limitations imposed by the dimensions of the ambient chamber in the tensile machine.

The observed behavior is similar to the elastic modulus development in solid-state drawing of polyethylene, which is determined by the absolute draw ratio. Irvine and Smith proposed a simplified model to predict the elastic modulus as a function of draw ratio under the assumption of pseudo-affine deformation [17]. This model describes the elastic modulus in the direction of tensile stretching, $\boldsymbol{E_{\|}}$, as the results of two elastic components: the "helix" component, $\boldsymbol{E_h}$, which is perfectly oriented in the stretching direction, and the "coil" component, $\boldsymbol{E_u}$, which is not oriented. The fraction of helix $\boldsymbol{f}$ is related to the distribution of angle between chain vector and drawing axis as follows in equation (3):

$$\left\langle \cos^2\theta \right\rangle = \frac{1+2f}{3} \tag{3}$$

This fraction of helix $\boldsymbol{f}$ is also related to the draw ratio $\boldsymbol{\lambda}$ according to equation (4):

$$f = \frac{3\lambda^3}{2\left(\lambda^3-1\right)}\left[1-\left(\lambda^3-1\right)^{-\frac{1}{2}}\tan^{-1}\left\{\left(\lambda^3-1\right)^{\frac{1}{2}}\right\}\right]-\frac{1}{2} \tag{4}$$

Under the assumption of uniform strain distribution, the elastic modulus of the specimen in the stretching direction is given by equation (5):

$$\frac{1}{E_{\|}} = \frac{f}{E_h} + \frac{1-f}{E_u} \tag{5}$$

Although being an oversimplified description of the actual structure, this model is in good agreement with experimental results at high draw ratios [17,18].

Henning showed a similar model to describe the physical properties of uniaxial stretched amorphous polymers [19]. In this model physical properties $\boldsymbol{a}$ are the properties represented by the second order tensor; for example, thermal expansion, linear compressibility or thermal resistivity. This model describes the physical properties of uniaxial stretched amorphous polymer by the properties of perfectly oriented material in the direction parallel ($\boldsymbol{a_1}$) and perpendicular ($\boldsymbol{a_2}$) to the chain axis.

$$a_{\|} = (a_1 - a_2)\left\langle \cos^2\theta \right\rangle + a_2 \tag{6}$$

$$a_{\perp} = \frac{1}{2}(a_1 + a_2) - \frac{1}{2}(a_1 - a_2)\left\langle \cos^2\theta \right\rangle \tag{7}$$

Here, $\boldsymbol{a}_{\|}$ and $\boldsymbol{a}_{\perp}$ represent the physical properties of the specimen in parallel and perpendicular to the stretching direction.

The following relationships hold for $\boldsymbol{a}_{\|}$, $\boldsymbol{a}_{\perp}$:

$$a_{\|} + 2a_{\perp} = 3a_0 \tag{8}$$

Table 1
In-plane average thermal conductivity of uniaxial stretched sample **PE_6_7**.

Rolling ratio	Stretching ratio (performed after rolling)	Total draw ratio	In-plane thermal conductivity (k_{ip}) (W/m K)
2.0	4.8	10	9.7
	6.8	14	12.7
	14	28	21.6
2.9	4.2	12	10.4
	7.6	22	19.0
	11	33	26.7
	13	38	27.5
4.1	2.3	9	9.6
	4.0	16	15.7
	7.3	29	23.1
	10	41	26.2
	14	57	31.7
5.3	2.0	11	10.4
	4.0	21	17.8
	6.4	34	26.4
	10	53	31.0
5.8	–	6	4.4
	5.7	33	23.8
	10	58	32.0
	13	75	36.2
	16	93	39.1
	21	120	44.2
6.5	24	160	44.3
	34	220	51.5

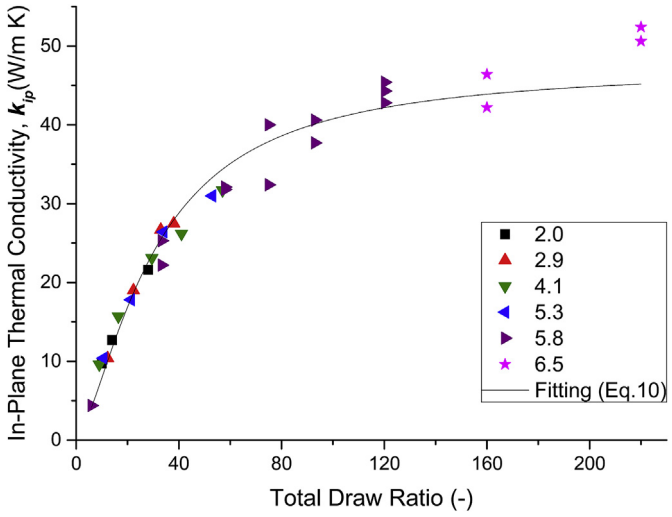

Fig. 3. In-plane thermal conductivities values as a function of TDR. Data from different rolling ratios are represented by different symbols. Each data point is averaged over 5 analyses. At higher draw ratios (>80), sampling from different points of the same specimen brings values that may differ of ±10% due to non-uniformity in stretching.

$$a_1 + 2a_2 = 3a_0 \tag{9}$$

where $\boldsymbol{a_0}$ is the property in the isotropic material.

By substituting $\boldsymbol{a}$ in equation (6) by the thermal resistivity $\boldsymbol{1/k}$ (with $\boldsymbol{1/k_1}$ for the direction parallel and $\boldsymbol{1/k_2}$ for the direction perpendicular to the chain direction) and incorporating equations (3) and (4), equation (10) can be obtained:

$$\frac{1}{k_{\|}} = \left(\frac{1}{k_1} - \frac{1}{k_2}\right)\left[\frac{\lambda^3}{\lambda^3 - 1} - \frac{\lambda^3}{\left(\lambda^3 - 1\right)^{\frac{3}{2}}}\tan^{-1}\left\{\left(\lambda^3 - 1\right)^{\frac{1}{2}}\right\}\right] + \frac{1}{k_2} \tag{10}$$

When fitting this equation with experimental values (black line in Fig. 3), we found a good agreement at lower draw ratios, and the fitting gives values of 0.45 W/m K for $\boldsymbol{k_2}$ and 47 W/m K for $\boldsymbol{k_1}$. We should consider that Hennig's model has been formalized for an amorphous system, so this can account for the deviation that we observe when going to higher draw ratios where crystal extension can be realized.

However, the increase in thermal conductivity seems to show two separate regimes, with a steep increase at ratios below 40, and a second, although less steep, increase after 80. This behavior is similar to the one we have previously observed for the tensile strength and tensile modulus of uniaxially drawn tapes of disentangled UHMWPE [8]. In that case, we ascribed the result to the initial crystal orientation followed by chain extension: this effect was particularly visible on the tensile strength, when UHMWPEs of

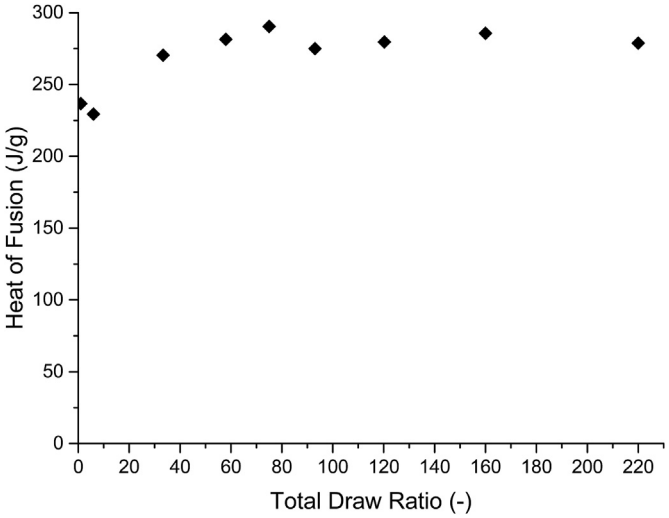

Fig. 4. Heat of Fusion of **PE_6_7** against TDR. Sample with rolling ratios of 5.8 and 6.5 are used except for TDR of 1, which is the value of the as-synthesized sample. The increase in heat of fusion and the chain orientation is further confirmed by the solid state NMR studies reported in Ref. [8] (see Fig. 4 of reference).

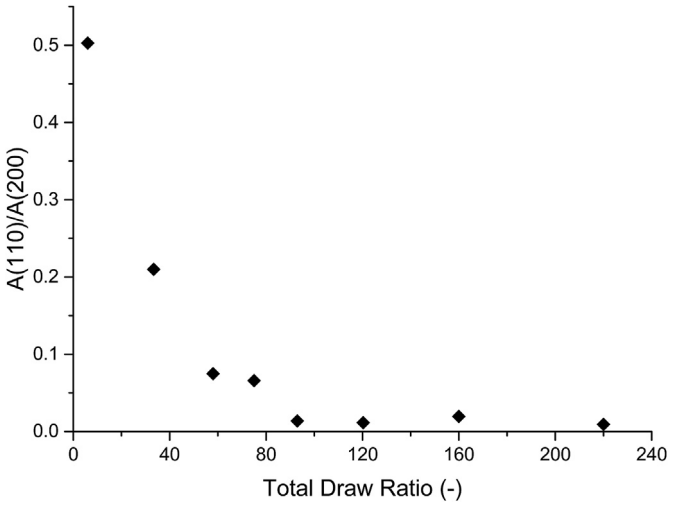

Fig. 5. The area ratio of (110) reflection and (200) reflection versus TDR.

different molecular weights were compared, as longer chains were entering the plateau at higher draw ratios and higher values of strength were reached.

When considering the thermal conductivity, it should be mentioned that, as we have previously reported (Fig. 4 of Ref. [8]), the crystallinity changes only slightly when going from the nascent sample to the specimens stretched at draw ratios of 40.

DSC experiments on uniaxial stretched samples show values of heat of fusion that increase from 230 J/g for a rolled sample to over 270 J/g for TDR of 40, as shown in Fig. 4, corresponding to an increase in crystallinity from 78% to over 92%, when crystallinities are calculated simply by dividing the heat of fusion with the literature value of 293 J/g [20]. Although the change of crystallinity is not significant at low draw ratios, the thermal conductivity increases from ~0.3 W/m K to 10 W/m K at draw ratios of just 10. This significant change can be attributed to the orientation of crystals along with the non-crystalline domains.

It is well known that crystal orientation parallel to the drawing direction develops at the early stage of stretching and it is nearly constant at high draw ratio (>10) [21]. However, further drawing gives significant improvement of material properties, which is attributed to the chain extension. Moreover, solid-state processing of nascent UHMWPE powder gives UHMWPE tapes with high crystal orientation in the planar direction. The intensity ratio of (110) diffraction peak against (200) diffraction peak has been evaluated by XRD and plotted in Fig. 5. It is evident that the 110/200 intensity ratio drops significantly for TDR up to 80 and then decreases slightly by further stretching, suggesting that the crystal orientation in axial and planar direction is almost complete by a TDR of 80.

After the 30-fold increase in thermal conductivity at the beginning of drawing, mainly driven by crystal orientation and chain extension, a further increase is realized, reaching 50 W/m K for this sample at draw ratios of 220. The latter increase in thermal conductivity at higher draw ratios could be attributed to the influence of apparent increase in crystal size along the draw direction: the crystal size dependence of thermal conductivity has been already mentioned by Choy [22]. However, in the macroscopic sample the presence of chain ends, in combination with crystal dimension along the chain length, are likely to influence the flow of phonons (Fig. 6).

Considering that the number of chain ends and crystal size are dependent on the molecular characteristics and higher order structure of the polymer used, molar mass, molar mass distribution and entangled states are likely to be important parameters influencing the thermal conductivity of the polymer.

For this reason, we decided to compare the thermal conductivity of UHMWPEs of different molecular weights as a function of the total draw ratio (TDR). To reach high values of TDR, a rolling ratio of about 6 was used in all cases. The calculated average values of thermal conductivity are reported in Table 2.

The values of thermal conductivity calculated for the three samples at various TDRs are plotted in Fig. 7. Similar to the observations on the tensile strength [14], the highest thermal conductivity is achieved for **PE_10_7** at a draw ratio of 200. The highest value of 65 W/m K is ~30% lower than that reported by Shen et al. [5], however it should be taken into account that in their case the

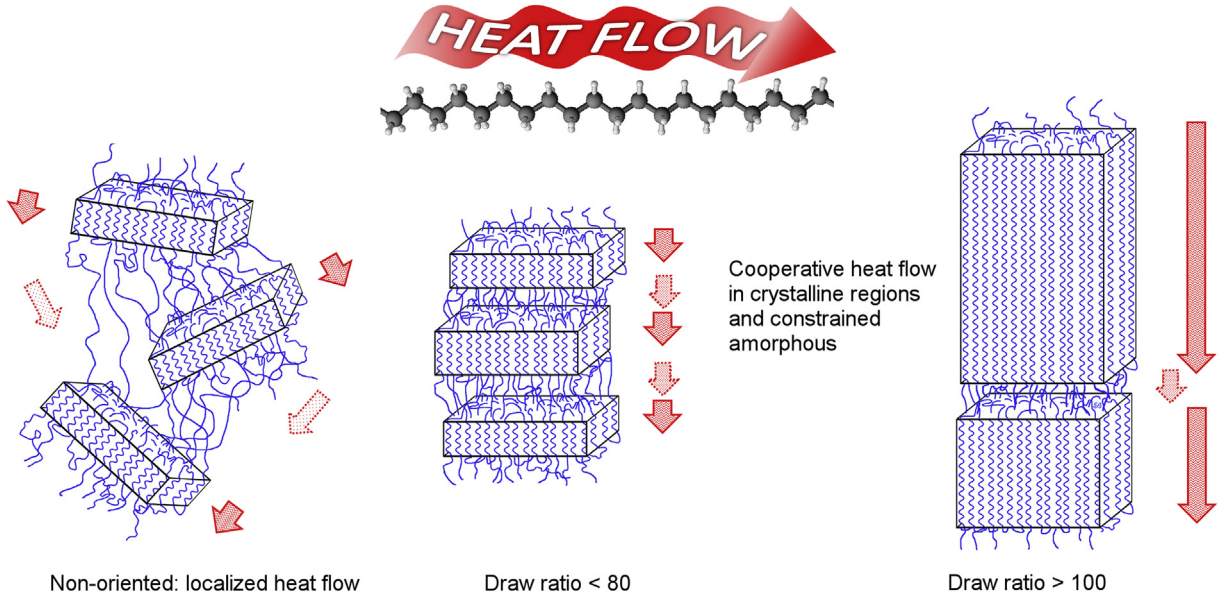

Fig. 6. The observed increase of thermal conductivity in the oriented material can be ascribed to crystal orientation for draw ratios lower than 80, followed by increase in crystal size at higher stretching [23,24].

Table 2
In-plane average thermal conductivity of uniaxial stretched samples **PE_2_4, PE_6_7, PE_10_7**.

Sample	Total draw ratio	In-plane thermal conductivity (k_{ip}) (W/m K)[a]
PE_2_4	6	4.3
	24	19.8
	52	26.7
	73	31.7
	94	37.8
	120	42.3
	160	42.8
	200	44.7
PE_6_7	6	4.4
	33	23.8
	58	32.0
	75	36.2
	93	39.1
	120	44.2
	160	44.3
	220	51.5
PE_10_7	6	4.8
	24	19.8
	32	25.2
	51	32.8
	65	37.3
	81	40.0
	98	39.5
	120	38.7
	140	46.8
	170	49.0
	200	65.0
	240	61.8

[a] Standard deviations for 5 analyses on the same sample are within ±5%. Standard deviations for different sampling locations are within ±10%.

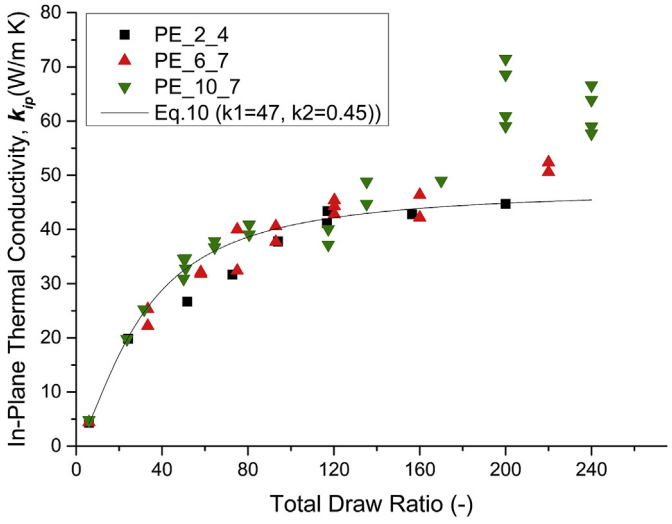

Fig. 7. In-plane thermal conductivity as a function of draw ratios for UHMWPEs of different molecular weights. Each data point is averaged over 5 analyses. At higher draw ratios (>80), sampling from different points of the same specimen brings values that may differ by ±10% due to non-uniform stretching. Data at high rolling ratios for **PE_6_7** are reported again for comparison.

values referred to a nanoscale segment of a fibre, while our values refer to the macroscopic aggregates of extended oriented crystals, where the presence of microvoids and air pockets cannot be excluded.

In fact, Choy et al. [25] have shown similar values of conductivities for solid state drawn samples of UHMWPE, but in that case the maximum value of thermal conductivity reached by stretching a single-mat UHMWPE to a draw ratio above 200 was 40 W/m K, while a solution-spun sample could only reach to the maximum value of 30 W/m K. The cause for the lower value of thermal conductivity in the solution spun fibers, compared to the solid-state processed tapes, can be attributed to the higher crystal plane orientation in the tapes compared to the fibers coupled with the higher molecular weight of the sample used in our study, resulting in a lower number of chain ends [8].

The influence of molecular weight on the structure development can be appreciated when comparing the intensity ratios of (110) and (200) reflection. As shown in Fig. 8, the lowest molecular weight sample **PE_2_4** gives the higher value of intensity ratio, which means lower crystal planar orientation, than the other samples. The low crystal planar orientation of **PE_2_4** can be the result of inefficient orientation caused by the higher density of entanglements, an occurrence we have previously discussed [9]. This result is in agreement with the observation that **PE_2_4** shows the lower thermal conductivity among all the samples considered.

The through-plane thermal conductivity (perpendicular to the draw direction) drops from 0.4 W/m K to 0.2 W/m K at the TDR of 40, and it decreases only slightly at higher TDRs. These results are qualitatively consistent with earlier work on the anisotropy of thermal conductivity in stretched samples of HDPE [26].

In addition to uniaxial stretching, disentangled UHMWPE offers the unique opportunity to perform biaxial stretching in the solid state [8]. The sample **PE_6_7** is processed through biaxial stretching, as described in Ref. [8], and the thermal conductivity is measured. The results are reported in Table 3.

The observed thermal conductivity in the isotropically aligned crystals of the biaxial drawn films is indeed surprising, as the value of 18.4 W/m K is similar to stainless steel, and to our knowledge this behavior has not been reported before. The high thermal conductivity in the biaxial drawn films having thickness of 30 μm can be attributed to the extended chain orientation in the biaxial direction, thus facilitating the flow of phonons.

It should be mentioned that the uni-axial orientation brings extremely high strength and modulus in the direction of drawing, but the tapes tend to fibrillate very easily. The fibrillation process increases with the decreasing polydispersity. This fibrillation is not observed in bi-axially stretched membranes, thus constituting a significant mechanical advantage compared to tapes.

Further morphological studies on the biaxial drawn films are

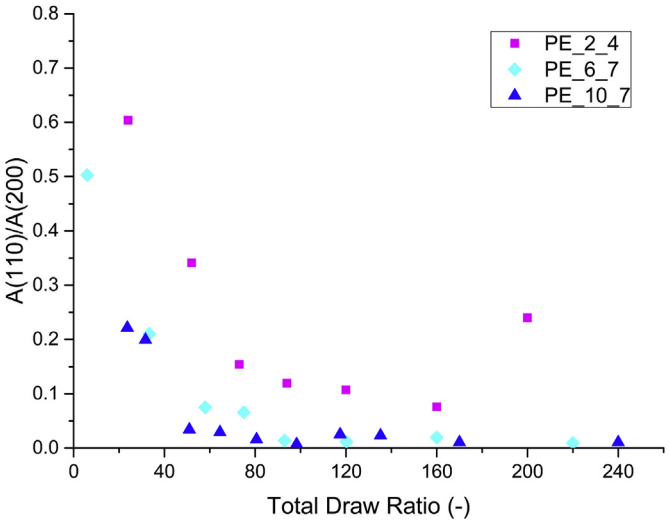

Fig. 8. The area ratio of (110) reflection and (200) reflection versus TDR. Data at high rolling ratios for **PE_6_7** are reported again for comparison.

Table 3
In-plane thermal conductivity of biaxial stretched **PE_6_7**.

Rolling ratio	Stretching ratio[a]	Ratio of areas after/before stretching	In-plane thermal conductivity (k_{ip}) (W/m K)
1.3 × 1.3	2.8 × 2.9	14	9.8
1.4 × 1.4	3.8 × 3.2	23	18.4

[a] The values have been determined from the grid lines traced on the sample before stretching.

under investigation and will be addressed in future publications.

4. Conclusions

UHMWPE with reduced number of entanglements can be oriented through uniaxial and biaxial stretching in the solid state without using any solvent. The high degree of chain orientation and the presence of extended chains have been associated with the exceptionally high tensile modulus and tensile strength of the drawn samples [14]. In this paper, we have addressed the ability of these oriented extended chains to conduct thermal energy through lattice vibration in an electrically-insulating polymer. In the uniaxially drawn tapes, the initial steep increase of thermal conductivity, from 0.3 W/m K to 10 W/m K for a total draw ratio of just 10, is ascribed to orientation of crystals, followed by chain (and crystal size) extension at higher draw ratios. For the first time, we have also reported on the relatively high thermal conductivity of 18.4 W/m K (similar to stainless steel) for a solid-state bi-axial stretched UHMWPE.

The most significant advantage offered by disentangled UHMWPE is the possibility to directly process the nascent material in the solid state to achieve macroscopic structures that are electrically insulating but thermally conductive in a range of in-plane thermal conductivity spanning from 10 to 60 W/m K, a feature that can be of use in any electrical application where dissipation of heat is required.

Conflict of interest

None.

Acknowledgments

The authors wish to thank David Hitt for his assistance in the use of the bi-axial stretching equipment. Funding: This project has been funded by the Engineering and Physical Science Research Council (EPSRC), grant EP/K034405/1.

References

[1] Z. Han, A. Fina, Thermal conductivity of carbon nanotubes and their polymer nanocomposites: a review, Prog. Polym. Sci. 36 (2011) 914–944, http://dx.doi.org/10.1016/j.progpolymsci.2010.11.004.
[2] C.-W. Nan, G. Liu, Y. Lin, M. Li, Interface effect on thermal conductivity of carbon nanotube composites, Appl. Phys. Lett. 85 (2004) 3549–3551, http://dx.doi.org/10.1063/1.1808874.
[3] T.R. Anthony, W.F. Banholzer, J.F. Fleischer, L. Wei, P.K. Kuo, R.L. Thomas, R.W. Pryor, Thermal diffusivity of isotopically enriched C12 diamond, Phys. Rev. B 42 (1990) 1104–1111, http://dx.doi.org/10.1103/PhysRevB.42.1104.
[4] A.G. Gibson, D. Greig, M. Sahota, I.M. Ward, C.L. Choy, Thermal conductivity of ultrahigh-modulus polyethylene, J. Polym. Sci. Polym. Lett. Ed. 15 (1977) 183–192, http://dx.doi.org/10.1002/pol.1977.130150401.
[5] S. Shen, A. Henry, J. Tong, R. Zheng, G. Chen, Polyethylene nanofibres with very high thermal conductivities, Nat. Nanotechnol. 5 (2010) 251–255, http://dx.doi.org/10.1038/nnano.2010.27.
[6] C. Lu, S.W. Chiang, H. Du, J. Li, L. Gan, X. Zhang, X. Chu, Y. Yao, B. Li, F. Kang, Thermal conductivity of electrospinning chain-aligned polyethylene oxide (PEO), Polym. U. K. 115 (2017) 52–59, http://dx.doi.org/10.1016/j.polymer.2017.02.024.
[7] J.B.P. Soares, J.D. Kim, G.L. Rempel, Analysis and control of the molecular weight and chemical composition distributions of polyolefins made with metallocene and Ziegler–Natta catalysts, Ind. Eng. Chem. Res. 36 (1997) 1144–1150, http://dx.doi.org/10.1021/ie960479x.
[8] S. Rastogi, Y. Yao, S. Ronca, J. Bos, J. Van Der Eem, Unprecedented high-modulus high-strength tapes and films of ultrahigh molecular weight polyethylene via solvent-free route, Macromolecules 44 (2011) 5558–5568, http://dx.doi.org/10.1021/ma200667m.
[9] A. Pandey, Y. Champouret, S. Rastogi, Heterogeneity in the distribution of entanglement density during polymerization in disentangled ultrahigh molecular weight polyethylene, Macromolecules 44 (2011) 4952–4960, http://dx.doi.org/10.1021/ma2003689.
[10] D.J. Hitt, M. Gilbert, A machine for the biaxial stretching of polymers, Polym. Test. 13 (1994) 219–237, http://dx.doi.org/10.1016/0142-9418(94)90029-9.
[11] W.N. Dos Santos, P. Mummery, A. Wallwork, Thermal diffusivity of polymers by the laser flash technique, Polym. Test. 24 (2005) 628–634, http://dx.doi.org/10.1016/j.polymertesting.2005.03.007.
[12] W.J. Parker, R.J. Jenkins, C.P. Butler, G.L. Abbott, Flash method of determining thermal diffusivity, heat capacity, and thermal conductivity, J. Appl. Phys. 32 (1961) 1679–1684, http://dx.doi.org/10.1063/1.1728417.
[13] U. Gaur, B. Wunderlich, Heat capacity and other thermodynamic properties of linear macromolecules. II. Polyethylene, J. Phys. Chem. Ref. Data 10 (1981) 119–152, http://dx.doi.org/10.1063/1.555636.
[14] S. Ronca, G. Forte, H. Tjaden, S. Rastogi, Solvent-free solid-state-processed Tapes of ultrahigh-molecular-weight polyethylene: influence of molar mass and molar mass distribution on the tensile properties, Ind. Eng. Chem. Res. 54 (2015) 7373–7381, http://dx.doi.org/10.1021/acs.iecr.5b01469.
[15] T. Kanamoto, A. Tsuruta, K. Tanaka, M. Takeda, R.S. Porter, Super-drawing of ultrahigh molecular weight polyethylene. 1. Effect of techniques on drawing of single crystal mats, Macromolecules 21 (1988) 470–477, http://dx.doi.org/10.1021/ma00180a032.
[16] L.H. Wang, S. Ottani, R.S. Porter, Two-stage drawing of high-molecular-weight polyethylene reactor powder, in: Polymer (Guildf), 1991, pp. 1776–1781, http://dx.doi.org/10.1016/0032-3861(91)90362-M.
[17] P.A. Irvine, P. Smith, Development of the axial Young's modulus with draw ratio of flexible-chain polymers, Macromolecules 19 (1986) 240–242, http://dx.doi.org/10.1021/ma00155a038.
[18] Y. Dirix, T.A. Tervoort, C.W.M. Bastiaansen, P.J. Lemslra, Solid-state drawing of polyethylenes: the pseudo-affine deformation scheme and aggregate models revisited, J. Text. Inst. 86 (1995) 314–321, http://dx.doi.org/10.1080/00405009508631336.
[19] J. Hennig, Anisotropy and structure in uniaxially stretched amorphous high polymers, J. Polym. Sci. Part C Polym. Symp. 16 (1967) 2751–2761, http://dx.doi.org/10.1002/polc.5070160528.
[20] B. Wunderlich, G. Czornyj, A study of equilibrium melting of polyethylene, Macromolecules 10 (1977) 906–913, http://dx.doi.org/10.1021/ma60059a006.
[21] P. Gao, M.R. Mackley, T.M. Nicholson, Development of anisotropy in ultra-high molecular weight polyethylene, Polym. Guildf. 31 (1990) 237–242, http://dx.doi.org/10.1016/0032-3861(90)90112-C.
[22] C.L. Choy, Y. Fei, T.G. Xi, Thermal conductivity of gel-spun polyethylene fibers, J. Polym. Sci. Part B Polym. Phys. 31 (1993) 365–370, http://dx.doi.org/10.1002/polb.1993.090310315.
[23] V.M. Litvinov, J. Xu, C. Melian, D.E. Demco, M. Moeller, J. Simmelink, Morphology, chain dynamics, and domain sizes in highly drawn gel-spun ultrahigh molecular weight polyethylene fibers at the final stages of drawing by SAXS, WAXS, and 1H Solid-State NMR, Macromolecules 44 (2011) 9254–9266, http://dx.doi.org/10.1021/ma201888f.
[24] N.A.J.M. Van Aerle, A.W.M. Braam, A structural study on solid state drawing of solution-crystallized ultra-high molecular weight polyethylene, J. Mater. Sci. 23 (1988) 4429–4436, http://dx.doi.org/10.1007/BF00551941.
[25] C.L. Choy, Y.W. Wong, G.W. Yang, T. Kanamoto, Elastic modulus and thermal conductivity of ultradrawn polyethylene, J. Polym. Sci. Part B Polym. Phys. 37 (1999) 3359–3367, http://dx.doi.org/10.1002/(SICI)1099-0488(19991201)37:23<3359::AID-POLB11>3.0.CO;2-S.
[26] C.L. Choy, W.H. Luk, F.C. Chen, Thermal conductivity of highly oriented polyethylene, Polym. Guildf. 19 (1978) 155–162, http://dx.doi.org/10.1016/0032-3861(78)90032-0.